

## Spin-Wave Resonance Studies in Invar Films\*

C. A. Bauer and P. E. Wigen

*Department of Physics, Ohio State University, Columbus, Ohio 43210*

The technique of spin-wave resonance has been employed to experimentally determine the spin-wave dispersion coefficient  $D$  for different compositions of nickel in iron. The results of this investigation indicate that for the fcc alloys (nickel-rich), the spin-wave dispersion coefficient decreases from its room-temperature value of  $3.8 \times 10^{-27}$  erg cm<sup>2</sup> at 60-at. % Ni in Fe to a minimum of  $2.7 \times 10^{-27}$  erg cm<sup>2</sup> at 45-at. % Ni in Fe. It then rises to a maximum of  $6.5 \times 10^{-27}$  erg cm<sup>2</sup> at the Invar point, 27-at. % Ni in Fe. The spin-wave dispersion coefficient for the bcc alloy (iron-rich) taken at room temperature decreases linearly from its value of  $5.0 \times 10^{-27}$  erg cm<sup>2</sup> at pure iron to a value of  $2.7 \times 10^{-27}$  erg cm<sup>2</sup> at the Invar point. The shape of both the bcc and fcc plots are in agreement with a plot constructed from data obtained using the technique of small-angle neutron scattering. The Landé  $g$  factor has also been determined as a function of composition of nickel in iron. For the bcc material,  $g$  is a constant at 2.20 in the range 22–31-at. % Ni in Fe. For the fcc material,  $g$  varies from its value of 2.15 in the region 42–60-at. % Ni in Fe to a value of 1.79 at 33-at. % Ni in Fe and then rises to 2.00 near the Invar point. The complex spin-wave patterns that are often detected in Invar thin films of mixed crystalline structure have been attributed to the different magnetizations associated with each of the crystalline phrases.

## INTRODUCTION

A number of intriguing physical and magnetic properties appear in the Invar region of the iron-nickel alloy system having the compositional range of 27–36-at. % Ni in Fe. These include a low coefficient of thermal expansion,<sup>1</sup> a decrease in the magnetic moment,<sup>1</sup> and large values of the resistivity and volume magnetostriction (positive).<sup>1</sup> Associated with these anomalies is a change in the crystalline structure, with a corresponding change in the lattice parameter, from bcc (iron-rich) to fcc near the Invar point 27-at. % Ni in Fe. Although many investigators have examined and attempted to explain the unusual properties of Invar,<sup>1,2</sup> a complete understanding of the Invar problem has yet to be achieved.

The most enigmatic property of this region, and yet potentially the most significant for the study of the stability of the ferromagnetic ground state, is the decrease of the magnetic moment per atom in the (fcc) alloy with decreasing nickel concentration. The magnetic moment per atom in the fcc material decreases at a rate closely related to the valency of the solute element, whereas in the bcc region the magnetic moment per atom remains independent of the solute concentration and constant at  $2.2 \mu_B$  (Bohr magnetons).<sup>3</sup>

Most interesting among the existing theoretical solutions to the Invar problem<sup>4–6</sup> is the suggestion by Shimizu<sup>7,8</sup> that ferromagnetism may be extended into the region where the Stoner criterion appears to be violated. This extension is possible since the density-of-states curve does not in reality vary as smoothly with energy as Stoner<sup>9</sup> had assumed, but rather has many peaks and valleys. Depending on

the position of the Fermi level in the topology of the density-of-states curve, it can be shown that the ferromagnetic state may have a lower energy than the paramagnetic state even though Stoner's criterion is violated. Applying this correction to the Stoner model, Shimizu and Hirooka<sup>8</sup> have asserted that the decrease in the magnetic moment near the Invar point is a manifestation of the Shimizu extended theory of ferromagnetism.

Of special significance to the understanding of the Invar problem were a series of small-angle neutron diffraction studies of spin-wave energies in Invar samples performed by Hatherly *et al.*<sup>10</sup> In both the fcc and bcc phases the spin-wave dispersion coefficient  $D(E = Dk^2$ , where  $E$  is the energy of a spin-wave with wave vector  $k$ ) has a linear dependence upon concentration, though with different slopes. Unfortunately, the results were obtained only for compositions from 100–40-at. % Ni in Fe, but when the curve is extrapolated to the Invar point a positive minimum value of  $D$  is obtained.

As a result of these investigations Katsuki and Wohlfarth<sup>11,12</sup> proposed another explanation for the instability of the ferromagnetic ground state at the Invar point. Using the theoretical relationship derived for  $D$  assuming a cubic lattice<sup>13</sup> the possibility was demonstrated, depending on the number of effective electrons per atom, that  $D$  could be zero or negative. Hence the hypothesis was proffered that the stability of the ferromagnetic ground state can be related to the sign of  $D$ .

In view of the argument of Katsuki<sup>12</sup> concerning the stability of the ferromagnetic ground state for iron-nickel alloy at the Invar point, a more detailed study of the behavior of the spin-wave dispersion coefficient would be helpful. Using the technique

of spin-wave resonance in thin films, the dependence of  $D$  on composition in both crystalline phases of Fe-Ni alloys and a study of the magnetic properties of Invar thin films were undertaken.

### THEORY

The equation of motion<sup>14</sup> for a thin film having a magnetization  $\vec{M}(z, t)$  oriented normal to the direction of the static magnetic field  $\vec{H}_0$  is described by

$$\frac{1}{\gamma} \frac{d\vec{M}}{dt} = \vec{M} \times \vec{H}_{\text{eff}}, \quad (1)$$

where  $\gamma$  is the gyromagnetic ratio and the effective magnetic field  $\vec{H}_{\text{eff}}$  is defined as

$$\vec{H}_{\text{eff}} = \vec{H}_0 - \hat{k} 4\pi [\vec{M}(z, t) \cdot \hat{k}] + (2A/M) \nabla^2 \vec{M}(z, t). \quad (2)$$

The spatial component of the magnetization  $\vec{M}(z, t)$  is given by

$$\vec{M}(z) = m_x \hat{i} + m_y \hat{j} + M(z) \hat{k},$$

where the components  $m_x$  and  $m_y$  are small compared to  $M(z)$  which is approximately equal to the saturation magnetization  $M$ . The spin-wave stiffness constant  $A$  in Eq. (2) is a measure of the strength of the exchange interaction between electron spins.

Using the volume inhomogeneity model developed by Portis<sup>15</sup> and Wigen *et al.*,<sup>16</sup> the spatial component of the internal field  $4\pi M(z)$  is defined as

$$4\pi M(z) = 4\pi M(0) (1 - 4\epsilon z^2/L^2), \quad (3)$$

with  $\epsilon$ , the parameter describing the inhomogeneity across the film thickness, defined as

$$\epsilon = \frac{4\pi M(0) - 4\pi M(\frac{1}{2}L)}{4\pi M(0)}. \quad (4)$$

In this model the spins are assumed to be pinned by a volume effect rather than a surface effect, i. e., the spins are free.

Defining the circularly polarized magnetization as  $m^* = m_x + im_y$ , and assuming a time dependence of the form  $e^{-i\omega t}$ , Eq. (1) reduces to

$$\frac{d^2 m^*}{dz^2} + \frac{1}{2A/M} \left( \frac{\omega}{\gamma} - H_0 + 4\pi M(0) - \frac{4\epsilon}{L^2} 4\pi M(0) z^2 \right) m^* = 0. \quad (5)$$

The solutions to Eq. (5) are complex but they can be approximated in two regions. If the magnetic field separation between the high-field mode occurring at  $H_0$  and some  $n$ th mode at  $H_n$  is such that

$$H_0 - H_n < 4\pi M(0) - 4\pi M(\frac{1}{2}L),$$

the magnetic field separation will be linear and given by

$$H_0 - H_n = n [(4\epsilon/L)(2A/M) 4\pi M(0)]^{1/2}.$$

When the field separation  $H_0 - H_n$  becomes greater than the parabolic variation in the internal field  $4\pi M(0) - 4\pi M(\frac{1}{2}L)$  the magnetic field separation between the modes becomes quadratic;

$$H_A - H_n = \frac{D}{g\mu_B} \left( \frac{\pi}{L} \right)^2 (n^2 - n'^2). \quad (6)$$

The spin-wave dispersion coefficient  $D$  is related to the spin-wave stiffness constant  $A$  by the relation  $2A/M = Dg\mu_B$ , where  $\mu_B$  is the Bohr magneton and  $g$  is the Landé  $g$  factor.

Experimentally, the spin-wave stiffness constant  $A$  and the inhomogeneity parameter can be determined by plotting the log of the field separation versus the log of  $n$ , and finding the point where the linear slope and the quadratic slope intersect.

The spin-wave dispersion coefficient  $D$  has been computed theoretically from the band model by Izuyama and Kuobo<sup>13</sup> assuming a simple cubic lattice and tight binding. They obtain

$$D = \frac{I_{\text{eff}}}{3N} \sum_k \left( \frac{f_k^+ + f_k^-}{2\Delta} \nabla_k^2 \epsilon_k - \frac{f_k^+ - f_k^-}{\Delta^2} (\nabla_k \epsilon_k)^2 \right), \quad (7)$$

where  $I_{\text{eff}}$  is the effective interaction between electrons,  $\Delta$  is the exchange splitting parameter given by  $\Delta = nI_{\text{eff}}\Gamma$ ,  $\Gamma$  is proportional to the magnetization and is given by  $\Gamma = \sum_k (f_k^+ - f_k^-)/nN$ ,  $N$  being the number of atoms,  $n$  the number of electrons per atom,  $\epsilon_k$  the single-particle energy, and  $f_k^{\pm}$  the Fermi function for the spin-up and spin-down states. This calculation is based on several critical assumptions: (i) The magnetic electrons are distributed in a single nondegenerate band; (ii) the effective exchange interaction between the electrons is a short-range interaction, here denoted by  $I_{\text{eff}}$ ; (iii) the value of the interaction energy appearing in the formula for  $D$  is essentially the same as that entering another theoretical formula of the theory, i. e., Stoner's criterion in the form

$$I_{\text{eff}} N(\epsilon) > 1.$$

According to Katsuki<sup>12</sup> an instability in  $D$  occurs at the Invar point. This instability is illustrated by an inspection of Eq. (7). Because of the periodicity of the Brillouin zones, the first term of this expression is zero and the second may be positive or negative depending on the Fermi levels of the spin-up and -down states. If  $I_{\text{eff}}$  is strong enough to induce strong ferromagnetism, and if the spin-up band is filled while the spin-down band is empty, then the second term is negative as  $f_k^+ - f_k^- = 1$  and  $(\nabla_k \epsilon_k)^2 > 0$ . Thus  $D$  may be zero or negative if the value of  $n$  (the number of electrons per atom) fills the upper subband of the  $3d$  band.

In the iron-group metals and alloys, the density-of-states curve has a sharp minimum at the posi-

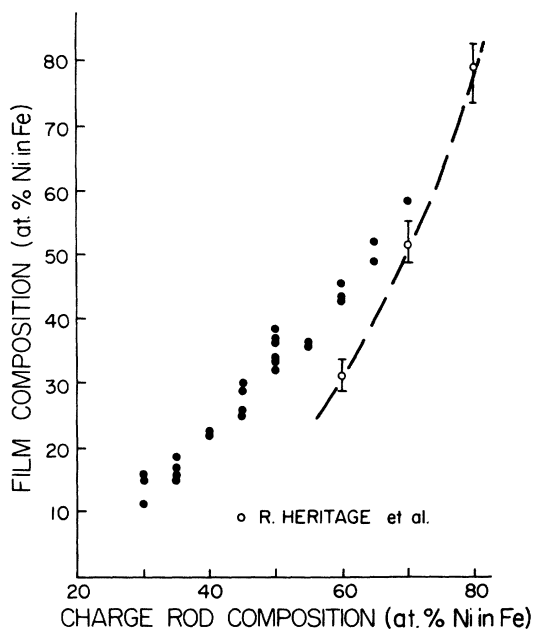


FIG. 1. Film composition (final) vs charge rod composition. (Electron bombardment heated the source.)

tion corresponding to the Fermi energy of Cr. At this position the upper part of the band has a capacity for four electrons. Assuming the number of  $4s$  electrons is 0.6, then the alloy 30-at.% Ni in Fe has just two holes in the  $3d$  band and just half fills the upper subband of the  $3d$  band. By applying the case of a single band [Eq. (7)] to the upper  $3d$  band, Katsuki expects that  $D$  will be negative for the 30-at.% Ni in Fe alloy and the ferromagnetic ground state will be unstable.

#### Magnetic Properties of Invar Films

The magnetic properties of ferromagnetic thin films are closely related to the techniques employed during their deposition. In order to deposit films with predetermined magnetic properties it is necessary to determine what effect variations in the substrate temperature, flatness of substrate, deposition rate, temperature of melt, and vacuum pressure will have on the resulting magnetic properties of the films. Though the effect of these variables on the resulting magnetic properties of Permalloy have been carried out in some detail,<sup>17</sup> they have yet to be reported for Invar.

The clarity of a spin-wave resonance spectrum has been shown to depend on the substrate surface as a result of the detailed studies of Prosen *et al.*<sup>18</sup> The present investigation suggests that ultraflat quartz ( $\sim 50\text{\AA}$  between peaks and valleys) of 2-mm thickness will minimize the effect of substrate surface flatness on the resultant spin-wave spectrum. Ultraflat quartz of lesser thickness appears to in-

troduce stresses attributable to substrate bending.

Although the phenomenon of iron enrichment does not seem to play a significant role during the deposition of Permalloy films,<sup>17,19</sup> it is significant for Invar films. The curve of Fig. 1 indicates the final composition of material deposited on a thin film when charge rods of varying compositions of nickel in iron are heated by means of electron bombardment. The results of this investigation are, in general, in agreement with those of Heritage *et al.*<sup>17</sup> whose data are indicated by the dashed line in Fig. 1.

The amount of iron enrichment for iron-nickel alloys in the Invar region decreases when a deposition rate in the range between 4 and 12  $\text{\AA}/\text{sec}$  is employed. In Heritage's results for Permalloy material the enrichment increases for rates of deposition below 5  $\text{\AA}/\text{sec}$ , but the decrease for higher rates of deposition is considerably slower than for Invar alloys (Fig. 2). Electron bombardment in both of these investigations heated the source.

The crystalline structure of the Invar films over the compositional range 12–60-at.% Ni in Fe was investigated by means of an x-ray diffractometer. The results of this investigation revealed that films with compositions richer in nickel than 42 at.% were invariably of the fcc structure, while those with nickel less than 25 at.% were bcc. In the Invar region, 27–38-at.% Ni in Fe, both crystalline structures usually were detected.

Films having the range of compositions produced by charge rods of 45-at.% Ni in Fe and 50-at.%

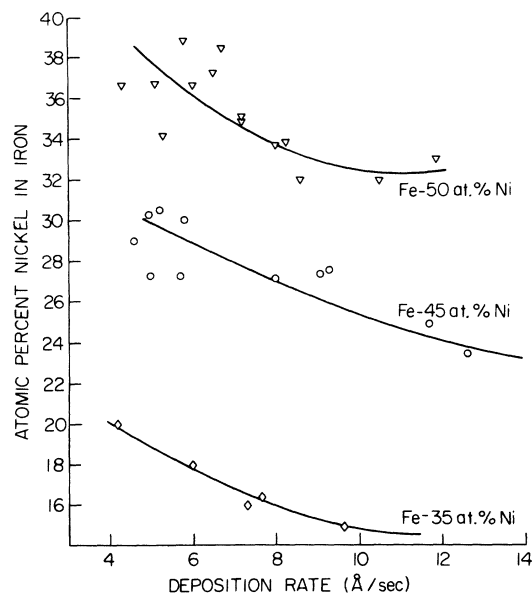


FIG. 2. Iron enrichment in the deposition of Invar thin films as a function of the deposition rate. (Electron bombardment heated the source.)

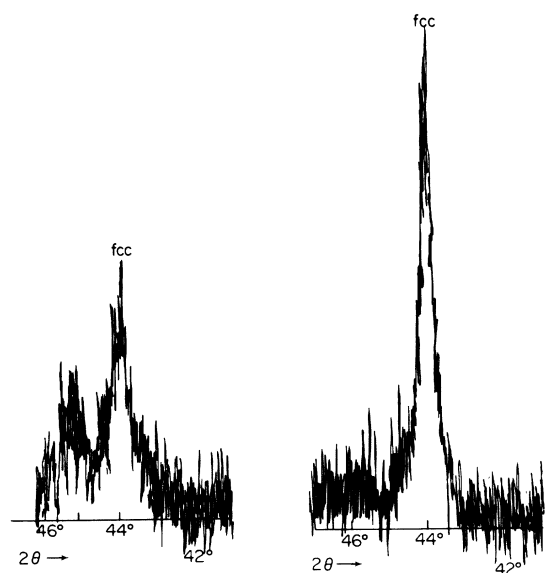


FIG. 3. X-ray diffraction data, Co source, showing (a) film IC 30D (40-at. % Ni in Fe) with no gold layer and (b) film IC 30B with a layer of gold (190 Å).

Ni in Fe are expected to produce Invar samples having a mixed crystalline structure. Since some of the films produced were entirely fcc or bcc, the role played by substrate temperature, deposition rate, or incident power in the production of these films would be worthy of comment. The results of these investigations, however, indicate that no relation exists between these parameters that would consistently give rise to a single phase structure in the Invar region.

The fcc phase may be stabilized in the Invar region, however, by depositing a thin layer of gold (~250 Å) before deposition of Invar. This stabilization may be attributed to the fcc structure of gold with a lattice constant nearly equal to that of iron-nickel fcc alloy in this region (3.58 Å) and the larger atomic radius and mass of gold. Although aluminum has a lattice constant almost equal to that of gold, a layer of aluminum did not produce the same orientation of the iron-nickel alloy, perhaps because of the smaller atomic radius and mass of the aluminum atoms.

X-ray studies of films which had been deposited with gold prior to the deposition of Invar showed enhanced fcc structure. Those films deposited with Invar at the same time without a gold coating generally were of dual crystalline structure with the fcc phase always much less intense than the gold Invar films (Fig. 3). Although a bcc peak was occasionally present for the gold-Invar films made from a 45- or 40-at. % Ni in Fe charge rod, this was expected<sup>2</sup> since the resulting iron-nickel composition of films (Fig. 1) is more favorable for

the deposition of bcc iron-nickel than fcc (Fig. 4).

#### Experimental Results

X-ray diffraction studies of Invar films used in these investigations suggest that a mixture of crystalline phases exists in the range of compositions 22–38-at. % Ni in Fe. Because the magnetization of the bcc structure is different from that of the fcc phase, it is expected that the spin-wave resonance patterns of films in this region will be complex with patterns due to the bcc phase superimposed on those due to the fcc phase.

With the magnetic field oriented normal to the surface of a film (the perpendicular case) the spin-wave spectrum of a dual crystalline phase film is characterized by two intense distinct peaks, one having a spin-wave structure associated with it and the other not (Fig. 5). In the parallel orientation a single broad peak is most often observed.

It is possible that a superimposed spectrum might result from the film having nonuniform thickness or stresses. This suggestion<sup>20</sup> did not prove productive for the interpretation of the phenomenon of the superimposed spin-wave spectrum. Several films were broken in half, in thirds, and on one film all the Invar was etched away except for a small dot (~1.5 mm diam.). The results were consistently the same (Fig. 6), the spin-wave spectrum remained unchanged, although reduced in

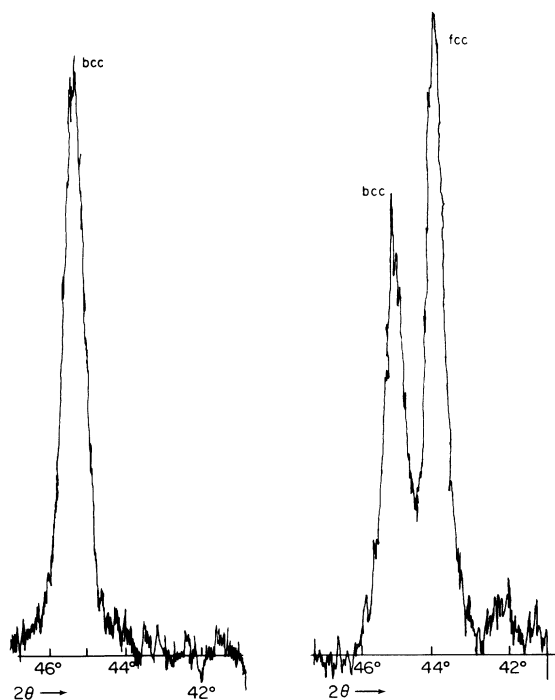


FIG. 4. X-ray diffraction data, Co source, showing (a) film IC 35E (29-at. % Ni in Fe) with no gold layer, and (b) film IC 35B with a thin layer of gold (430 Å).

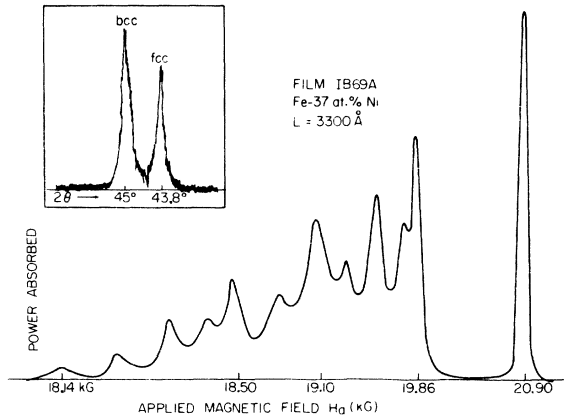


FIG. 5. Plot of the spin-wave spectrum of film IB 69A.

intensity.

Hansen<sup>2</sup> reported that annealing iron-nickel samples in the Invar region will result in the stabilization of the fcc phase. The amount of conversion to fcc depends on the composition of the film and on the temperature and duration of the anneal.

In order to investigate the effect of annealing on the crystalline structure and spin-wave spectrum of films in this region a number of films were annealed to 400 °C for 15 min in a high vacuum.

The spin-wave spectra of film IB 69A (37-at. % Ni in Fe) illustrate a typical reaction to the effect of annealing for this period of time. Before the anneal (Fig. 5) a clear spectrum is associated with the 19.90 kG peak, and no spectrum is associated with the 20.90-kG peak. After the anneal (Fig. 7) a broad intense peak has formed at 17.17 kG, the spin-wave pattern has become unclear, and the field position of the 20.90-kG peak has remained relatively stable. The x-ray diffraction data confirm a stabilization of the fcc structure (compare

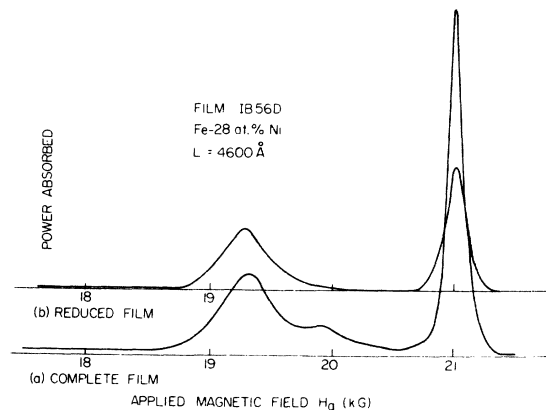


FIG. 6. Plot of the spin-wave spectrum of film IB 56D before (a) and after (b) the film was reduced to a small dot 1.5 mm diam.

insets).

The spin-wave spectra of this film and the others tested indicate that a significant change had occurred in the crystalline phase which gave rise to the structured peak. As a result of annealing, though not as apparent in the IB 69A film (Fig. 7) as in others, there is a decrease in the relative intensity of the nonstructured peak. Associated with these effects is the marked increase in the fcc crystalline phase, and the increased magnetic homogeneity of the annealed films.

Since the increase in the magnetic homogeneity of the film and the stabilization of the fcc phase is dependent on the time of anneal, several films were annealed to 400 °C for 1 h. The results of this heat treatment are tabulated in Table I. All of these films, with the exception of IB 41B and IB 56C, have been entirely converted to fcc (Fig. 8) and their spin-wave spectra show a single peak, with little or no spin-wave structure. The magnetization and field position of this remaining structure suggest that it was once associated with the structured peak in the nonannealed data.

As a result of this hour-long anneal the structure of film IB 69A has become substantially fcc and the lack of spin-wave resonance for the 17.17-kG mode suggests that the magnetic properties of the film are homogeneous. Comparing this data to that taken after annealing for 15 min, it is possible to associate the 17.17-kG mode with the magnetization of the fcc structure.

Since annealing does disrupt the spectrum associated with the structured pattern in mixed phase films and since the amount of fcc phase increases with annealing, the structured pattern in these films appears to be associated with the fcc phase. Hence the nonstructured peak, from the critical-angle experiment, must be attributed to the magnetization due to the bcc phase.

The magnetization of a thin film depends not only

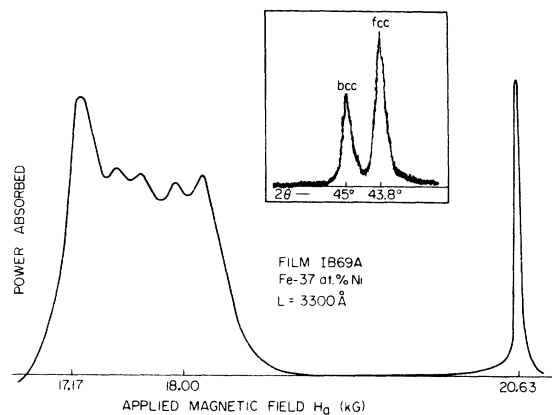


FIG. 7. Plot of the spin-wave spectrum of film IB 69A after a 15 min anneal at 400 °C in a high vacuum.

TABLE I. Effect of 1-h anneal on spin-wave resonance data of ferromagnetic thin films in Invar region.

Film	at. % Ni in Fe	Phase	Thickness	Before anneal perpendicular kG	After anneal perpendicular kG	Before internal field kG	After internal field kG
IB 56C	27.8	bcc	4550	22.30	22.10	19.50	19.18
IB 56C	27.8	fcc	4550	20.71	20.51	17.68	17.50
IB 41B	31.9	bcc	3090	21.40	20.72	18.02	17.39
IB 41B	31.9	fcc	3090	16.88	16.29	13.80	13.36
IB 80D	35.6	fcc	2660	19.19	16.45	16.11	13.17
IB 68A	36.6	fcc	2950	20.38	17.10	17.31	14.04
IB 68D	36.6	fcc	2950	20.23	16.79	17.14	13.64
IB 69A	36.6	fcc	3270	19.91	17.17	16.82	14.16
IB 70A	37.2	fcc	2810	19.45	17.28	16.98	14.24
IB 72B	38.8	fcc	2950	19.37	18.19	16.25	15.08

on the composition, but also on the temperature. For fcc material, Crangle and Hallam<sup>3</sup> have plotted the reduced magnetization  $M/M_0$  versus the reduced temperature  $T/T_C$ , where  $T_C$  is the Curie temperature, for several compositions. Because the Curie temperature for the bcc material is greater than that of the fcc material of the same composition, the reduced temperature  $T/T_C$  will be less than that of the fcc material. Hence, for a reduction in temperature a greater change in magnetization is expected for the fcc material than for the bcc.

In order to observe the change in the magnetization, which is proportional to the change in the field position of the  $k=0$  mode, with a decrease in temperature, several films having good dual spectra, but of different composition, were chosen. The results of this temperature study are displayed in Table II.

These shifts in the  $k=0$  mode, which occur as a result of a decrease in temperature, verify that the peak associated with the structure belongs to the fcc phase and the peak with no visible spin-wave pattern belongs to the bcc phase. Since the composition of IB 41C, 32-at. % Ni in Fe, has a smaller

Curie temperature for the fcc phase than film IB 70C, 37-at. % Ni in Fe, a greater net shift for the  $k=0$  mode position for the fcc material and a lesser net shift for the bcc material is to be expected.

During the course of these investigations experiments indicated that a thin layer of gold (~250 Å) deposited before the deposition of Invar greatly enhanced the stability of the fcc structure. Using this technique Invar thin films of only fcc structure were deposited to 28-at. % Ni in Fe. The single upfield peak, whose origin is attributed to the presence of bcc material in Invar films, was conspicuously absent from the spin-wave resonance data of films with gold.

The spin-wave resonance spectra used to determine the data points for the plots of the Landé  $g$  factor and the values of the spin-wave dispersion constant were taken from films whose structure was shown by x-ray diffraction studies to be only fcc or bcc. Although spin-wave resonance patterns containing dual  $k=0$  peaks possessed  $D$  values in agreement with the trend of the plot, they were excluded in order to remove all ambiguity.

The Landé  $g$  factor has been plotted in Fig. 9 for

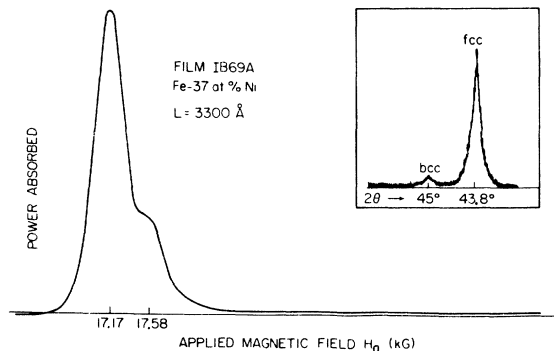


FIG. 8. Plot of the spin-wave spectrum of film IB 69A after a 1 h anneal at 400 °C in a high vacuum.

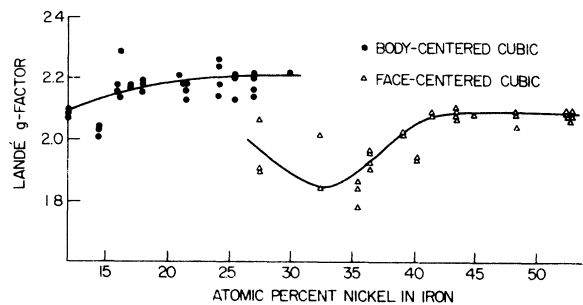


FIG. 9. Variation of the Landé  $g$  factor with composition.

TABLE II. Effect of reduction in temperature on field position of  $k = 0$  mode for perpendicular case.

Film	at. % Ni in Fe	Thickness Å	Perpendicular	Perpendicular	Change kG
			kG 300°K	kG 77°K	
IB 41C	31.9	3090	21.83	22.70	+0.87
IB 41C	31.9	3090	19.50	21.40	+1.90
IB 80C	35.6	2660	19.84	20.86	+1.02
IB 80C	35.6	2660	18.56	19.78	+1.22
IB 69C	36.6	3270	19.50	20.50	+1.00
IB 69C	36.6	3270	18.60	19.77	+1.77
IB 70C	27.2	2810	19.04	20.41	+1.37
IB 70C	27.2	2810	16.97	18.72	+1.75

both the fcc and bcc material. For the bcc region, the value of  $g$  is nearly constant at 2.18, but for the fcc structure the behavior is more interesting. In this region the value of  $g$  decreases near 42-at. % Ni in Fe from a constant value of 2.08 and reaches a minimum near 33-at. % Ni in Fe before increasing again.

In Fig. 10 the experimental results for the spin-wave dispersion coefficient  $D$  has been plotted for the fcc structure (pluses). The bcc structure (dots) has been plotted in Fig. 11.

The experimental plot (Fig. 12) of the internal field has been drawn as a function of composition for both crystalline phases. For the bcc phase (dots) the internal field is nearly constant before it begins to decrease near 22-at. % Ni in Fe and finally diminishes near 42-at. % Ni in Fe as the bcc structure becomes more unstable and the fcc phase is preferred.

In the fcc material (diamonds) the internal field at first obeys a smooth curve, then begins to increase in an irregular fashion. This scattered increase which begins at 38-at. % Ni in Fe may be attributed to the effect of residual and isotropic stress and the large value of the volume magnetostriction which is observed in this region.<sup>21</sup> This scattering arises from the great dependence of the

stress on the substrate temperature and rate of deposition.<sup>22</sup>

It is well known that annealing will reduce stresses and magnetic inhomogeneities which give rise to the appearance of the odd modes (the asymmetrical variation of the internal field with respect to the center of the film), altering of the lower modes (parabolic variation of the internal field), and, finally, pinning itself. For films of mixed phase, annealing promotes a conversion to the fcc phase. The resultant change is noted in the spectrum by a decrease in the intensity of the odd modes and the reduction of the effects of superimposed modes (Figs. 5-7).

Since the stresses and magnetostriction present in Invar films appear to reach a maximum near the Invar point, the resultant internal field determined for the fcc material at these compositions does not agree with the bulk  $4\pi M$  values given by Bozorth.<sup>1</sup> These magnetic inhomogeneities may be relieved by annealing, and several films having compositions in this region were annealed for an hour at 400°C.

The spectrum after anneal indicated that a magnetically homogeneous material has been produced since there is a single resonance peak with little

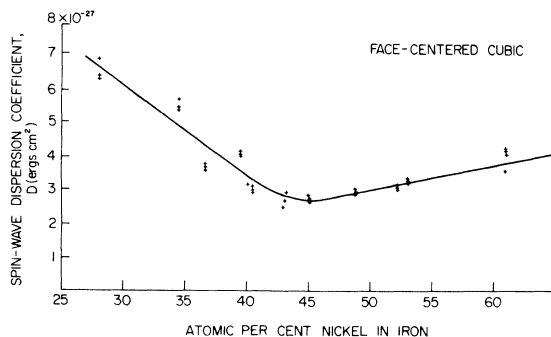


FIG. 10. Variation of the spin-wave dispersion coefficient  $D$  for the bcc crystalline structure with composition of nickel in iron.

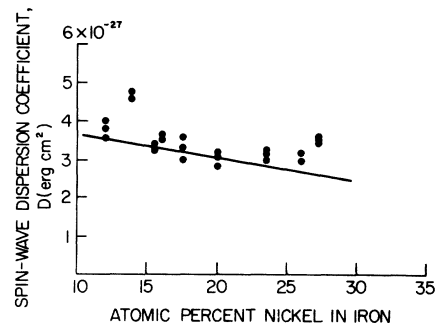


FIG. 11. Variation of the spin-wave dispersion coefficient  $D$  with composition of nickel in iron for the fcc crystalline structure.

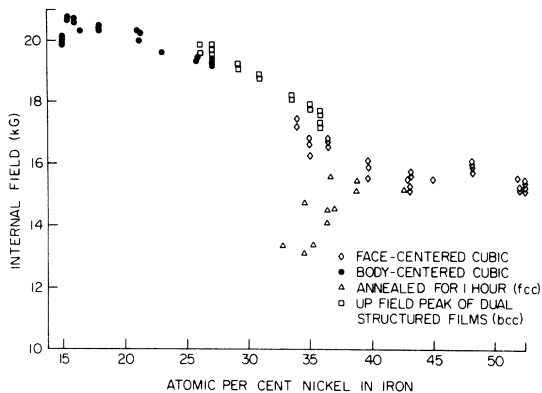


FIG. 12. Dependence of the internal field  $H_i$  with composition of nickel in iron.

or no spin-wave structure. Furthermore, x-ray diffractometer studies indicate the structure of these films has been converted to the fcc. The results of this study are tabulated in Table I and the new plot of the internal field, which represents the dependency of the magnetization for the fcc material (triangles) at 300 °K is plotted in Fig. 12.

### CONCLUSIONS

This investigation of the magnetic properties of iron-nickel thin films in the Invar region has revealed three important magnetic characteristics. It is possible to obtain spin-wave resonance from both of the crystalline structures present in dual crystalline phase Invar films, that the Landé  $g$  factor varies with composition for both of the crystalline structures, and that the spin-wave dispersion coefficient  $D$  for the fcc material increases as the Invar point, 27-at. % Ni in Fe, is approached, and is not zero at this point for the fcc phase as had been predicted.<sup>12</sup> Further, it has been shown that a thin layer of gold will greatly enhance the stability of the fcc structure for Invar films deposited from

material in the Invar region, and that iron enrichment is an important effect that must be considered when Invar material is to be deposited.

Anomalous peaks in spin-wave resonance spectra have been reported elsewhere,<sup>23</sup> but no attempt was made to explain their meaning or origin. Based on the results of a critical-angle study, the reaction of dual crystalline structured films to a decrease in temperature, and the variation of the internal field with composition suggest the observed peaks are separate and may be attributed to the bcc and fcc material present in the thin film. When a thin layer of gold is deposited prior to the deposition of Invar, it is possible to stabilize the fcc phase; the anomalous peak is notably absent from gold-Invar films.

A similar decrease of the Landé  $g$  factor with composition has been found by Bagguley<sup>24</sup> in his studies of iron-nickel-manganese colloidal suspensions. Since  $g$  is related to spin-orbit effects, the increase in the lattice parameter  $a$ , which occurs as the Invar point is approached,<sup>1</sup> might increase spin-orbit coupling and thereby decrease  $g$ .

The experimental plot of the bcc data for the spin-wave dispersion coefficient from spin-wave resonance data is slightly less than those obtained by Hatherly *et al.*<sup>10</sup> using the technique of small-angle neutron scattering. However, since Hatherly's results are extrapolated to 0 °K and since  $D$  has a similar dependence on temperature as does  $M$ , in thin-film spin-wave resonance experiments,<sup>25</sup> it is expected that his results would be slightly greater. For the fcc material the agreement between the two techniques is close, but no comparison can be made about the results after 40-at. % Ni in Fe since Hatherly's data end at that point.

Near the Invar point the sharp increase of  $D$  for the fcc phase is clearly unfavorable to the argument of Katsuki.<sup>12</sup> The thrust of this investigation is such as to discount a zero value of the spin-wave dispersion coefficient  $D$  as the direct cause of decreasing magnetization at the Invar point.

\*Work supported by the National Science Foundation.

<sup>1</sup>R. Bozorth, *Ferromagnetism* (Van Nostrand, Boston, 1951).

<sup>2</sup>M. Hansen, *Constitution of Binary Alloys* (McGraw-Hill, New York, 1958).

<sup>3</sup>J. Crangle and C. Hallam, Proc. Roy. Soc. (London) **A272**, 119 (1963).

<sup>4</sup>E. Kondorsky and V. Sedov, J. Appl. Phys. **31**, 3315 (1960).

<sup>5</sup>S. Chikazumi, T. Mizoguchi, N. Yamaguchi, and P. Beckwith, J. Appl. Phys. **39**, 939 (1968).

<sup>6</sup>R. Weiss, Proc. Phys. Soc. (London) **82**, 281 (1963).

<sup>7</sup>M. Shimizu, Proc. Phys. Soc. (London) **84**, 397 (1964), Paper I; **85**, 147 (1965), Paper II; A. Katsuki, Phys. Letters **8**, 7 (1964).

<sup>8</sup>M. Shimizu and S. Hirooka, Phys. Letters **27A**, 530

(1968).

<sup>9</sup>E. Stoner, Proc. Roy. Soc. (London) **A165**, 373 (1938).

<sup>10</sup>M. Hatherly, K. Minakawa, R. Lowde, J. Mallett, M. Stringfellow, and B. Torrie, Proc. Phys. Soc. (London) **84**, 55 (1964).

<sup>11</sup>A. Katsuki and E. Wohlfarth, Proc. Phys. Soc. (London) **295**, 182 (1962).

<sup>12</sup>A. Katsuki, Brit. J. Appl. Phys. **18**, 199 (1967).

<sup>13</sup>T. Izuyama and R. Kubo, J. Appl. Phys. **35**, 1074 (1964).

<sup>14</sup>P. E. Wigen, C. F. Kooi, and M. R. Shanabarger, J. Appl. Phys. **35**, 3302 (1964).

<sup>15</sup>A. Portis, Appl. Phys. Letters **2**, 69 (1963).

<sup>16</sup>P. E. Wigen, C. F. Kooi, M. R. Shanabarger, and T. Rossing, Phys. Rev. Letters **9**, 206 (1962); P. E. Wigen, C. F. Kooi, M. R. Shanabarger, U. Cummings,



and M. Baldwin, *J. Appl. Phys.* **34**, 1137 (1963).

<sup>17</sup>R. Heritage, A. Young, and I. Bolt, *Brit. J. Appl. Phys.* **14**, 439 (1963).

<sup>18</sup>R. Prosen, B. Gran, J. Kivel, C. Searle, and A. Morrish, *J. Appl. Phys.* **34**, 1147 (1963).

<sup>19</sup>C. Kennedy, Master's thesis (Ohio State University, Columbus, 1969).

<sup>20</sup>G. Bailey (unpublished).

<sup>21</sup>R. Spain, *Appl. Phys. Letters* **6**, 8 (1965).

<sup>22</sup>G. Weiss and D. Smith, *J. Appl. Phys.* **33**, 1166 (1962).

<sup>23</sup>Z. Frait and M. Ondris, *Czech. J. Phys. B* **11**, 885 (1961).

<sup>24</sup>D. Bagguley, *Proc. Phys. Soc. (London)* **B67**, 549 (1954).

<sup>25</sup>T. Phillips, *Proc. Roy. Soc. (London)* **A292**, 224 (1966).

PHYSICAL REVIEW B

VOLUME 5, NUMBER 11

1 JUNE 1972

## Temperature Dependence of Phonon Raman Scattering in $\text{FeBO}_3$ , $\text{InBO}_3$ , and $\text{VBO}_3$ : Evidence for a Magnetic Contribution to the Intensities

I. W. Shepherd\*

*Central Research Department, † E. I. du Pont de Nemours and Company,  
Experimental Station, Wilmington, Delaware 19898*

(Received 25 August 1971)

The complete Raman spectra comprised of  $4E_g$  and  $1A_{1g}$  modes have been observed in four materials of calcite structure (point group  $D_{3d}$ ) from 15 to 400 °K: ferromagnetic  $\text{VBO}_3$  ( $T_c = 32.5$  °K), antiferromagnetic  $\text{FeBO}_2$  ( $T_c = 350$  °K) and  $\text{Fe}_{0.9}\text{Ga}_{0.1}\text{BO}_3$  ( $T_c = 272$  °K), and nonmagnetic  $\text{InBO}_3$ . The energies of the modes are similar in all samples, with approximate values of  $930\text{ cm}^{-1}$  ( $A_{1g}$ ) and  $1210, 650, 400,$  and  $270\text{ cm}^{-1}$  ( $E_g$ ), and show no significant shift over the temperature range studied. Observed intensity variations with temperature of three lines in  $\text{InBO}_3$  relative to the  $A_{1g}$  symmetric mode are consistent with changes in phonon population with temperature. Large variations in intensity of lines relative to the  $A_{1g}$  modes were observed in the region of  $T_c$  which were qualitatively similar in all three magnetic materials. At high temperatures ( $T > 6T_c$ ) in  $\text{VBO}_3$  the intensity changes with temperature were consistent with phonon population changes. The intensity changes in the magnetic crystals are attributed to a phonon-magnon interaction arising from an exchange coupling which depends on ion position. No scattering from magnons was observed in the borates, but the temperature dependence of a line in the spectrum of the structurally related (point group  $D_{3d}$ ) transparent antiferromagnet  $\text{FeF}_3$  was characteristic of magnon scattering.

### I. INTRODUCTION

Recent scattering experiments on magnetic materials have demonstrated the influence of magnetic order on the phonon Raman spectrum.<sup>1,2</sup> The material studied in Ref. 2 was  $\text{FeBO}_3$  which is a transparent canted antiferromagnet having calcite structure (point group  $D_{3d}$ );<sup>3</sup> the materials studied in Ref. 1 were the semiconducting chalcogenide spinels,  $\text{CdCr}_2\text{Se}_4$  ( $T_c = 130$  °K) and  $\text{CdCr}_2\text{S}_4$  ( $T_c = 85$  °K), both of which are ferromagnetic and highly absorbing in the visible region of the spectrum.<sup>4-7</sup> Despite their very different physical properties, the Raman spectra in all these materials show similar significant intensity variations with temperature in the region of the Curie points. These intensity changes may possibly be attributed to an interaction between spin system and phonons.<sup>8</sup> Infrared absorption measurements in  $\text{CoF}_2$ , which also showed temperature-dependent intensities, were explained by an interaction between magnetic excitations and phonons<sup>9</sup>; other related papers<sup>10,11</sup> include the electron-hole interaction in discussions

of optical absorption in magnetic semiconductors.

The present work extends the study<sup>2</sup> of  $\text{FeBO}_3$  to two other materials,  $\text{VBO}_3$  and  $\text{InBO}_3$ , which have the same structure as  $\text{FeBO}_3$  while differing markedly in their magnetic properties. The small saturation magnetization of 2.07 emu/g in  $\text{FeBO}_3$  ( $T_c = 350$  °K) results from the canting of the two magnetic sublattices.<sup>3</sup> The much larger magnetization of 83.5 emu/g observed in  $\text{VBO}_3$  ( $T_c = 32.5$  °K) is equivalent to  $1.64\mu_B$  per  $\text{V}^{3+}$  ion.<sup>12</sup> Although this is smaller than the expected value of  $2\mu_B$  it does indicate that  $\text{VBO}_3$  is a true ferromagnet.  $\text{InBO}_3$  is, of course, nonmagnetic. There are two experimental advantages to dealing with these borate compounds. First, they are highly transparent to the exciting laser radiation which leads to excellent signal-to-noise ratios. Second, the calcite structure has a simple Raman spectrum of five allowed modes, one of symmetry  $A_{1g}$  and four  $E_g$ . All these are observed and easily identified in the crystals studied here. A comparison of the Raman spectra as a function of temperature in  $\text{FeBO}_3$  and  $\text{VBO}_3$  should cast some light on the